JOURNAL OF VIROLOGY, Nov. 2007, p. 12272–12284 Vol. 81, No. 22
0022-538X/07/$08.00+0 doi:10.1128/JVI.00984-07

Crystallographic and Biochemical Analysis of Rotavirus NSP2 with Nucleotides Reveals a Nucleoside Diphosphate Kinase-Like Activity▽

Mukesh Kumar,[1] Hariharan Jayaram,[1]† Rodrigo Vasquez-Del Carpio,[2]‡ Xiaofang Jiang,[1] Zenobia F. Taraporewala,[2] Raymond H. Jacobson,[3] John T. Patton,[2] and B. V. Venkataram Prasad[1]*

Verna and Marrs McLean Department of Biochemistry and Molecular Biology, Baylor College of Medicine, One Baylor Plaza, Houston, Texas 77030[1]; Laboratory of Infectious Diseases, NIAID, National Institutes of Health, Bethesda, Maryland 20892[2]; and Department of Biochemistry and Molecular Biology, University of Texas, M. D. Anderson Cancer Center, Houston, Texas 77030[3]

Received 7 May 2007/Accepted 20 August 2007

Rotavirus, the major pathogen of infantile gastroenteritis, carries a nonstructural protein, NSP2, essential for viroplasm formation and genome replication/packaging. In addition to RNA-binding and helix-destabilizing properties, NSP2 exhibits nucleoside triphosphatase activity. A conserved histidine (H225) functions as the catalytic residue for this enzymatic activity, and mutation of this residue abrogates genomic double-stranded RNA synthesis without affecting viroplasm formation. To understand the structural basis of the phosphatase activity of NSP2, we performed crystallographic analyses of native NSP2 and a functionally defective H225A mutant in the presence of nucleotides. These studies showed that nucleotides bind inside a cleft between the two domains of NSP2 in a region that exhibits structural similarity to ubiquitous cellular HIT (*hi*stidine *t*riad) proteins. Only minor conformational alterations were observed in the cleft upon nucleotide binding and hydrolysis. This hydrolysis involved the formation of a stable phosphohistidine intermediate. These observations, reminiscent of cellular nucleoside diphosphate (NDP) kinases, prompted us to investigate whether NSP2 exhibits phosphoryl-transfer activity. Bioluminometric assay showed that NSP2 exhibits an NDP kinase-like activity that transfers the bound phosphate to NDPs. However, NSP2 is distinct from the highly conserved cellular NDP kinases in both its structure and catalytic mechanism, thus making NSP2 a potential target for antiviral drug design. With structural similarities to HIT proteins, which are not known to exhibit NDP kinase activity, NSP2 represents a unique example among structure-activity relationships. The newly observed phosphoryl-transfer activity of NSP2 may be utilized for homeostasis of nucleotide pools in viroplasms during genome replication.

Rotaviruses are the major cause of life-threatening diarrhea in children worldwide (13). The genome (~18 kb) of rotavirus consists of 11 segments of double-stranded RNA (dsRNA) encoding six structural and six nonstructural proteins (NSPs) (13). Several studies have shown that endogenous transcription of dsRNA segments, genome replication/packaging, and assembly of subviral particles take place in specialized compartments called viroplasms, which appear early during infection (30). NSP2, along with NSP5, is essential for the formation of these perinuclear, non-membrane-bound, electron-dense inclusions (14). Coexpression of NSP2 and NSP5 alone has been shown to be sufficient for the formation of viroplasm-like structures (14). NSP2 also appears to interact directly or indirectly with other structural proteins present in the viroplasm, such as VP2 (30), which forms the innermost capsid layer of the virion (32), and VP1, which is the viral RNA-dependent RNA polymerase (45).

Biochemical studies on recombinant NSP2 have shown that in addition to single-stranded-RNA (ssRNA)-binding and helix-destabilizing activities (42), NSP2 exhibits nucleotide triphosphatase (NTPase) activity (40). The protein cleaves the terminal phosphate from nucleotide triphosphates without any specificity for a particular base. Recent studies have shown similar triphosphatase activity with pppRNA as a substrate, establishing that NSP2 can be considered a 5′-RNA triphosphatase (RTPase) (46). How these various ligand-binding and enzymatic activities of NSP2 are utilized in the context of genome replication remains unclear.

Crystallographic analysis showed that NSP2, with two well-defined domains separated by a prominent cleft, forms a donut-shaped octamer with a 35-Å central hole and deep grooves lined by basic residues at the periphery (17). The C-terminal domain of the NSP2 structure displays surprising similarity to HIT (*hi*stidine *t*riad) proteins, despite the lack of any sequence homology and the signature HIT (His-X-His-X-His-XX) motif. The HIT proteins represent a family of ubiquitous cellular proteins with nucleotidyl hydrolase and transferase activities (6, 27). The central His residue in the HIT motif is important

* Corresponding author. Mailing address: Verna and Marrs McLean Department of Biochemistry and Molecular Biology, Baylor College of Medicine, One Baylor Plaza, Houston, TX 77030. Phone: (713) 798-5686. Fax: (713) 798-1625. E-mail: vprasad@bcm.tmc.edu.

† Present address: Howard Hughes Medical Institute and the Department of Biochemistry, Brandeis University, Waltham, MA 02454.

‡ Present address: Structural Biology Program, Department of Molecular Physiology and Biophysics, Mount Sinai School of Medicine, New York, NY 10029.

▽ Published ahead of print on 5 September 2007.

for catalytic activity. There are some important differences between NSP2 and HIT proteins. NSP2 specifically hydrolyzes the oxygen linkage between the β- and γ-phosphates of the nucleotide through a Mg^{2+}-dependent mechanism, whereas HIT proteins exclusively act on the linkage between the α- and β-phosphates in a Mg^{2+}-independent manner. These differences suggest that the mode of nucleotide binding and catalysis by NSP2 is distinct from that of the HIT proteins. Based on a structural comparison showing that H225 within the cleft of NSP2 superimposes with the catalytic histidine in HIT proteins, H225 was proposed as the catalytic residue of NSP2 (17). Subsequent mutational analysis has established that this residue is essential for the triphosphatase activity of NSP2 (8, 46). In vivo complementation studies with the enzymatically defective H225A and K188A mutants failed to promote dsRNA synthesis even though neither the octameric nature of NSP2 nor viroplasm formation (41) was affected. Thus, the triphosphatase activity of NSP2 is somehow linked to rotavirus genome replication.

The observation that NSP2 exhibits ssRNA-binding and helix-destabilizing activities along with NTPase activity prompted the suggestion that NSP2 might function as a molecular motor, utilizing the energy derived from NTP hydrolysis to facilitate rotavirus genome replication/packaging (35, 40). Several cellular and viral helicases use NTP hydrolysis as a source of energy to translocate bound nucleic acids (3, 26). For helicases, the NTPase activity of the enzyme is typically stimulated by the binding of nucleic acids to the protein, and NTP hydrolysis is accompanied by large conformational changes. However, for NSP2, binding of nucleic acid to the protein, if anything, reduces NTPase activity (46). Thus, how the NTPase activity of NSP2 is used in rotavirus genome replication is unclear.

We carried out crystallographic and biochemical studies on native NSP2 and the functionally defective H225A mutant in the presence of nucleotides to investigate how NSP2 interacts with nucleotides, the mechanism of NTP hydrolysis, and whether nucleotide binding is associated with conformational changes. These studies provide evidence that the NTPase activity of NSP2 is associated with a phosphoryl-transfer function similar to that seen for cellular nucleoside diphosphate (NDP) kinases. This activity may have a role in the homeostasis of nucleotides within the viral factories in which the rotavirus genome is replicated.

MATERIALS AND METHODS

Expression, purification, and crystallization. NSP2 was expressed in *Escherichia coli* strain SG13009(pREP4) and purified using Ni-nitrilotriacetic acid affinity chromatography as described previously (40). Crystals were obtained by the hanging-drop vapor diffusion method. Crystals of NSP2-nucleotide complexes were formed when protein (6 to 8 mg/ml) was mixed with nucleotides (0.6 to 1.0 mM) and then equilibrated against a reservoir solution containing 6 to 8% polyethylene glycol 10000 and 20 mM Tris-HCl (pH 7.5). These crystals were further soaked in 10 to 15 mM nucleotides for 2 days prior to being frozen in a cryoprotectant solution. Crystals of the H225A mutant without nucleotides were obtained under the conditions described earlier for preparing native NSP2 crystals (17).

Data collection and processing and refinement of the structure. Diffraction data from the frozen crystals were collected at 100 K on the ID-19 beamline at Advanced Photon Source and were processed using d*Trek (31). Data processing statistics are shown in Table 1. Structures of the NSP2–ATP-γS complex and the H225A mutant alone and as a complex with nucleotides were determined by molecular replacement using the software PHASER (28). Iterative cycles of model building and refinement were carried out using O (18) and CNS 1.1 (7), with a portion of the data (5%) set aside for validation. Refinement statistics are shown in Table 1.

Phosphorylation of NSP2. In vitro experiments showing the transfer of radiolabel from ATP–γ-^{35}S to NSP2 were performed using the same protocol as that described earlier (40). Briefly, reaction mixtures containing 2.0 μM NSP2, 50 mM Tris-HCl (pH 7.5), and 2.0 μM ATP–γ-^{35}S (1,250 Ci/mmol) (Perkin-Elmer) were incubated at 37°C for the indicated periods (see Fig. 2A). Phosphorylated NSP2 was detected by sodium dodecyl sulfate-polyacrylamide gel electrophoresis (SDS-PAGE) and autoradiography. As controls, identical reaction mixtures were set up, except that they lacked ATP–γ-^{35}S. After incubation, NSP2 in the mixtures was resolved by SDS-PAGE and detected by immunoblotting with anti-NSP2 polyclonal antisera (40).

Mass spectrometric analysis. Reaction mixtures containing 1.0 μM NSP2 and either 10.0 μM ATP–γ-S or 10.0 μM ATP in 10 mM Tris-HCl (pH 7.5) were incubated at 37°C for 4 h and then injected onto a Vydac 218MS5105 C_{18} column in a 0.02% trifluoroacetic acid–acetonitrile buffer system. The eluent from the column was directly infused into an Agilent LC-MSD TrapSL ion-trap mass spectrometer for electrospray ionization. Approximately 20 protonation states of NSP2 between 600 and 1,200 *m*/*z* were used for deconvolution analysis to determine the NSP2 mass after incubation with either ATP–γ-S or ATP.

Measurement of NDP kinase activity. The NDP kinase activity of NSP2 was analyzed using a real-time bioluminometric assay (19), a luciferin/luciferase system that detects ATP generation in reaction mixtures. An ATP bioluminescence assay kit containing luciferin, luciferase, and dilution buffers was purchased from Sigma. All reactions were carried out at either room temperature or 37°C in 20 mM Tris-HCl (pH 7.5), 4 mM $MgCl_2$, and different concentrations of ADP and NTPs. The pH of the solution was adjusted to 7.5 after mixing all the components. The reaction was initiated in a volume of 500 μl by the addition of NSP2 to a final concentration of 2 μM. One hundred microliters of this reaction mixture was mixed with 100 μl of 500-fold-diluted ATP assay mix from the kit, and the emitted light was measured using a Monolight 2010 luminometer (Analytical Luminescence Laboratory). The instrument was preset to integrate the amount of light produced over a 10-second interval without an initial delay. The concentration of ATP in the reaction mixture was determined from the intensity of emitted light by preparing an ATP standard calibration curve. Initial experiments showed a linear increase in the concentration of ATP over the first 60 min (see Fig. 6A). Hence, the velocity of the reaction was obtained from the concentrations of ATP in the reaction mixture at 0, 10, 20, 30, and 40 min. The control experiments showed that the recombinant NSP2 preparations were slightly contaminated with adenylate kinase, which is typical of proteins purified from a bacterial source. Accordingly, 5 μM of the adenylate kinase inhibitor Ap5A [P^1,P^5-di(adenosine-5′) pentaphosphate] was added initially to all reaction mixtures. However, later on, NSP2 was further purified using a cation-exchange column (Poros 20 HS; PerSeptive Biosystems) mounted on a high-performance liquid chromatography system. NSP2 eluted at 1.0 M NaCl in 20 mM Tris-HCl (pH 7.5) as a single Gaussian peak. The purified protein was dialyzed against 20 mM Tris-HCl (pH 7.5) and used in all kinetic experiments. The control experiments clearly showed that purified NSP2 had no contamination of adenylate kinase, and hence, Ap5A was not added in subsequent experiments, which are shown in Fig. 6. All of the kinetic data were analyzed using the program GraphPad Prism 4.

Protein structure accession numbers. The refined coordinates along with the structure factors have been deposited in Protein Data Bank with identification codes 2R7C, 2R7J, 2R7P, and 2R8F for NSP2 plus ATP-γ-S complex, H225A NSP2, H225A NSP2 plus AMPPNP complex, and H225A NSP2 plus ATP-γ-S complex, respectively.

RESULTS

Phosphorylation of NSP2 by ATP–γ-S. Our initial attempts to soak nucleotides into the crystals of native NSP2 previously grown in the presence of 100 to 200 mM magnesium were unsuccessful. Subsequently, filter binding assays revealed that the failure was due to the high concentrations of magnesium used in the crystallization buffers. Notably, filter binding assays indicated that concentrations higher than 3 to 4 mM decreased the binding of nucleotides to NSP2 exponentially. We then attempted to crystallize native NSP2 in the absence of any salts. Although the native protein could not be crystallized in the absence of salts, diffraction-quality crystals were readily

TABLE 1. Crystallographic data collection and refinement statistics

Parameter	Value[a]			
	NSP2 plus ATP–γ–S	H225A NSP2 plus ATP–γ–S	H225A NSP2 plus AMPPNP	H225A NSP2
Data collection				
Space group	I422	I422	I422	I422
Cell dimensions				
a, *b*, *c* (Å)	108.17, 108.17, 151.92	108.64, 108.64, 155.66	108.43, 108.43, 154.33	106.96, 106.96, 151.15
α, β, γ (°)	90.0, 90.0, 90.0	90.0, 90.0, 90.0	90.0, 90.0, 90.0	90.0, 90.0, 90.0
Resolution (Å)	50-2.7 (2.8-2.7)	50-2.8 (2.9-2.8)	50-2.8 (2.9-2.8)	50-2.6 (2.7-2.6)
R_{merge} (%)	6.6 (43.9)	8.0 (28.1)	11.2 (42.9)	6.2 (40.0)
$I/\sigma I$	17.1 (3.7)	14.9 (5.1)	13.0 (5.0)	15.2 (2.9)
Completeness (%)	98.2 (99.3)	99.2 (99.9)	99.9 (100)	99.9 (99.3)
Redundancy	7.55 (7.37)	7.81 (7.97)	13.82 (14.30)	8.01 (7.50)
Refinement				
Resolution (Å)	50-2.7	50-2.8	50-2.8	50-2.6
No. of reflections	11,690	11,718	11,643	13,859
R_{work}/R_{free}	0.225/0.278	0.216/0.271	0.222/0.263	0.226/0.278
No. of atoms				
Protein	2516	2498	2507	2494
Ligand/ion	4	31	21	
Water	15	99	47	60
B factors				
Protein	60.05	63.73	71.24	56.25
Ligand/ion	69.62	94.69	88.14	
Water	55.12	52.17	52.35	47.93
RMSD				
Bond lengths (Å)	0.0112	0.0069	0.0074	0.0071
Bond angles (°)	1.34	1.23	1.25	1.20

[a] Values in parentheses refer to the highest-resolution shell. The refined coordinates along with the structure factors have been deposited in Protein Data Bank.

obtained under salt-free conditions when the native protein was cocrystallized with nucleotides. These crystals diffracted to a resolution of 2.7 Å. NSP2 in the presence of ATP–γ-S crystallized in the same space group (I422) as the native protein, with one molecule in the crystallographic asymmetric unit forming a donut-shaped octamer with 4-2-2 crystallographic symmetry (Fig. 1A). Electron density maps showed a strong extra density very close to the N-ε of His225 in both the 2Fo-Fc

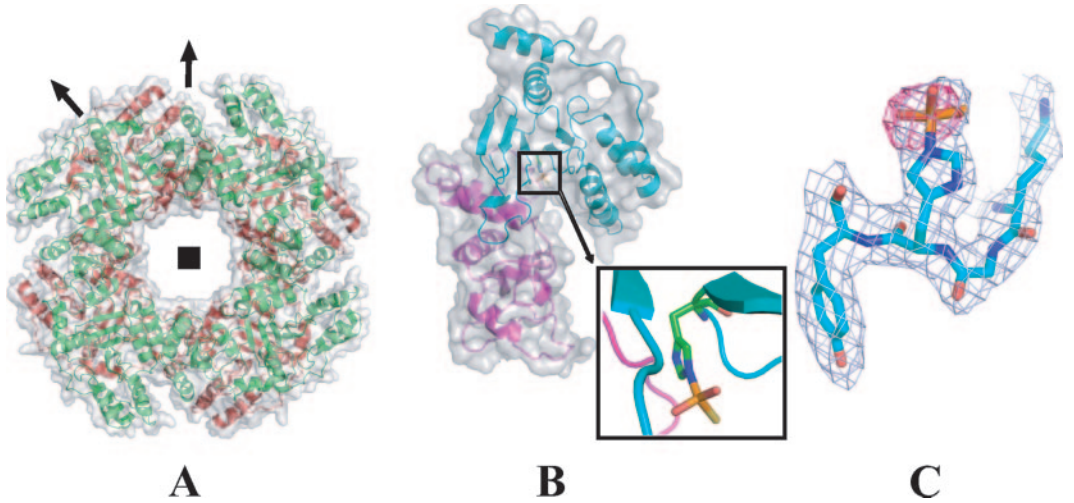

FIG. 1. Crystal structure of NSP2 with ATP–γ-S showing phosphorylation of His225. (A) NSP2 octamer, as viewed along the fourfold axis, shown in ribbon representation inside a semitransparent surface. Application of 4-2-2 crystal symmetry to the asymmetric unit, consisting of one NSP2 molecule, results in the formation of a donut-shaped octamer. For convenience of viewing, the two tetramers in the octamer are colored red and green. The fourfold and two twofold symmetry axes of the octamer are indicated by a filled square and two arrows, respectively. (B) NSP2 protomer showing phosphorylated His225 (in stick representation inside a square), located at the base of the cleft between the N- and C-terminal domains, which are colored magenta and cyan, respectively. (Inset) Close-up view of the phosphorylated His225 residue. (C) $2F_o$-Fc map contoured at 1.2σ (shown in light blue) and Fo-Fc map contoured at 3σ (shown in red), indicating the covalent attachment of a thiophosphoryl group to His 225.

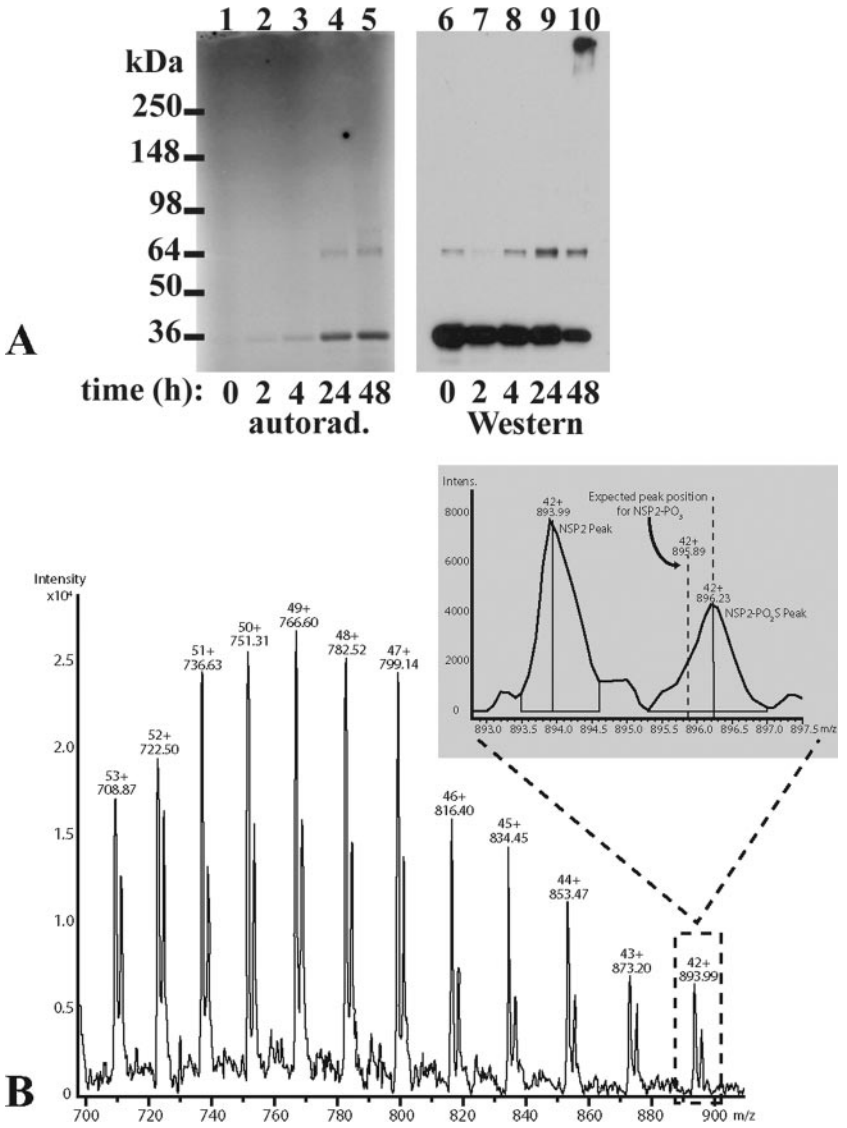

FIG. 2. Biochemical and mass spectroscopy analysis of NSP2 phosphorylation. (A) Transfer of radiolabel from ATP–γ-^{35}S to NSP2 as a function of time was analyzed by incubating 2 μM NSP2 in reaction mixtures containing 50 mM Tris-HCl (pH 7.5) and 2 μM ATP–γ-^{35}S, followed by SDS-PAGE and autoradiography (lanes 1 to 5). As a control, parallel reaction mixtures containing NSP2 but lacking ATP–γ-^{35}S were set up. NSP2 in the mixtures was resolved by SDS-PAGE and analyzed by Western blot assay, using guinea pig polyclonal anti-NSP2 antiserum and goat anti-guinea pig serum conjugated to horseradish peroxidase. Luminescence was detected with a Pierce SuperSignal West Pico chemiluminescence kit. (B) Electrospray ionization mass spectrum of the protein region generated by incubation of NSP2 with ATP–γ-S. Each peak in the protein region was resolved into two types of species, representing the native and phosphorylated forms of NSP2. A magnified portion of the spectrum about the +42 charge state shows the expected positions for peaks corresponding to thiophospho or phospho adducts of NSP2.

(>1σ) and Fo-Fc (>3σ) maps. This extra density could be fitted well with a phosphoryl group covalently attached to H225 inside the cleft of NSP2 (Fig. 1B and C), forming a thiophosphohistidine.

The formation of phosphohistidine indicates that NSP2 hydrolyzes ATP–γ-S, even though this is generally considered to be a nonhydrolyzable analogue of ATP. To confirm the cleavage of ATP–γ-S and the formation of the phosphoenzyme intermediate, we carried out biochemical and mass spectrometric analyses. NSP2 was incubated with radiolabeled ATP–γ-^{35}S for various lengths of time. Analysis of the reaction mixtures by gel electrophoresis followed by autoradiography revealed a band corresponding to radiolabeled monomeric NSP2 that generally increased in intensity during the 24- to 48-h incubation period (Fig. 2A). A minor amount of radiolabeled dimeric NSP2 was also detectable by the 24- and 48-h time points. Western blot assay indicated that NSP2 was remarkably stable during the 48-h incubation period, with some loss during the later times associated with the formation of insoluble aggregates not entering the gel (Fig. 2A). In sum, the radiolabeled moiety of ATP–γ-^{35}S was covalently transferred to NSP2 under Mg^{2+}-free conditions, albeit with slow kinetics. With both [γ-^{32}P]ATP and Mg^{2+} in the reaction mixture, instead of just ATP–γ-S, the phosphate transfer to NSP2 pro-

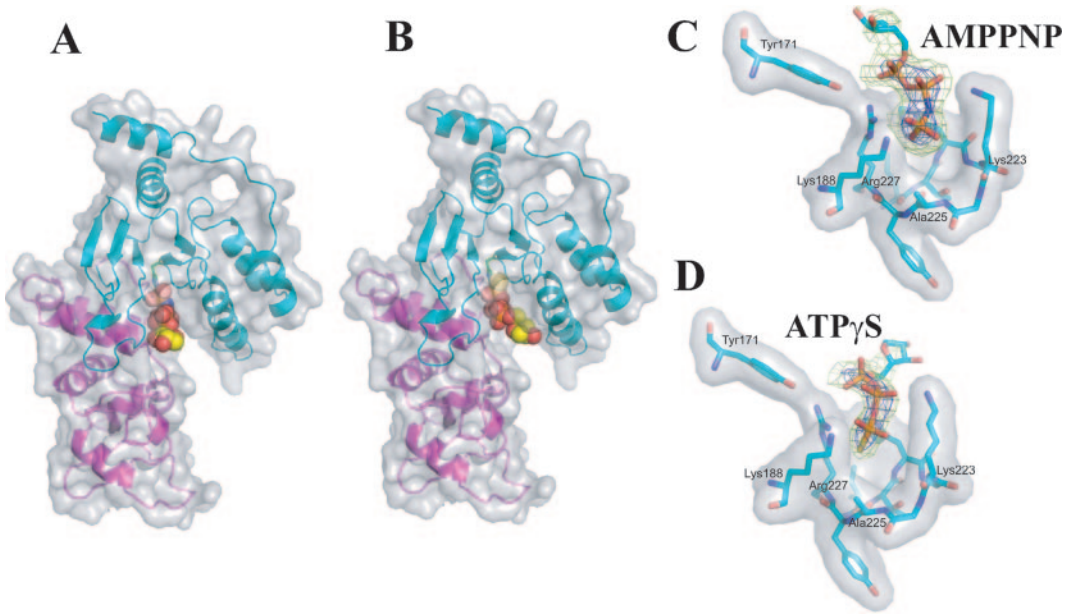

FIG. 3. Nucleotide binding to H225A NSP2 mutant. (A) Structure of H225A NSP2-AMPPNP complex. (B) Structure of H225A NSP2–ATP–γ-S complex. The H225A NSP2 mutant structure is shown in ribbon representation inside a semitransparent surface, with the N- and C-terminal domains colored magenta and cyan, respectively. The nucleotides bound in the cleft of the NSP2 monomer are shown as spheres. (C) Fo-Fc map contoured at 6σ and 2.5σ (blue and green, respectively) showing the presence of AMPPNP in the structure of the H225A NSP2-AMPPNP complex. (D) Fo-Fc map contoured at 4σ and 2.5σ (blue and green, respectively) showing the presence of ATP–γ-S in the structure of the H225A NSP2–ATP–γ-S complex.

ceeded more quickly. Specifically, whereas the γ-^{32}P moiety was detectably transferred to NSP2 in less than an hour, transfer of the γ-^{35}S label took several times longer (data not shown). However, with time, the intensity of the γ-^{32}P label associated with NSP2 decreased, perhaps due to hydrolysis of the phosphohistidine (8). With ATP–γ-S, the bound thiophosphate is retained longer because of the increased stability of the P-N linkage (between the γ-phosphate of the thiophosphate contributed by ATP–γ-S and the N-ε of the histidine side chain) due to lower electronegativity of the sulfur atom (25). The longer retention time has been advantageous for crystallographic visualization of phosphohistidine intermediates.

Further evidence showing that only the γ-thiophosphate of ATP–γ-S was transferred to the protein came from electrospray ionization mass spectrometry. In this experiment, NSP2 was incubated with ATP–γ-S and then subjected to liquid chromatography-mass spectrometric analysis. NSP2 eluted as a single chromatographic peak from a reversed-phase column and was sprayed into an ion-trap mass spectrometer. The resultant mass spectrum displayed a group of related peaks that corresponded to the different protonation states of NSP2 in the electrospray mixture (Fig. 2B). Each of these charge states was observed to split into a doublet, with peaks that corresponded to the unmodified or γ-thiophosphate adduct form of NSP2. Deconvolution analysis revealed the relative abundances of these species to be 1 to 0.7, with corresponding masses of 37,513.4 and 37,609.9 Da. The calculated mass of NSP2 from its sequence is 37,504.6 Da, which corresponds to the mass of one of the species (37,513.4 Da) within experimental error. The molecular mass of the modified form was 96 Da more than the first species, within error, and resulted from the covalent attachment of the γ-thiophosphate of ATP–γ-S to the protein. To confirm the transfer of the γ-thiophosphate, a second experiment was performed using normal ATP. In this case, no adduct could be observed to form on NSP2. The failure to observe an adduct with normal ATP was due to the inherent instability of phosphohistidine under the acidic conditions used for electrospray analysis. This strongly corroborated the 96-Da shift and mass identification of the thiophosphate as the moiety being transferred to NSP2. Although the nonthio form of phosphohistidine was not detectable, and thus mass spectrometry could not rule out transfer of the α- or β-phosphate, transfer of either the α- or β-phosphate from ATP by NSP2 would require a change of mechanism and stereochemistry from those observed with ATP–γ-S, which would be very improbable. Together, these experiments and the results from crystallographic analysis unambiguously indicate that NSP2 cleaves ATP–γ-S and that the γ-thiophosphate becomes covalently attached to His225. The phosphohistidine intermediate thus formed could result from the nucleophilic attack by the N-ε of His225 on the P-γ atom of ATP–γ-S, leading to the cleavage of the P-γ–O-β bond and the formation of the ADP product. The electron density for ADP, however, was not clearly seen in the crystal structure.

Nucleotide binding site in NSP2. To understand the mode of nucleotide binding and the mechanism of histidine phosphorylation, crystal structures of a mutant NSP2 protein containing a His225-Ala mutation (H225A) and of its complexes with ATP analogs were determined (Fig. 3). The overall structure of the H225A mutant is very similar to that of native NSP2, with a root mean square deviation (RMSD) of 0.42 Å for the matching C-α atoms. The structure of the H225A mutant shows clear

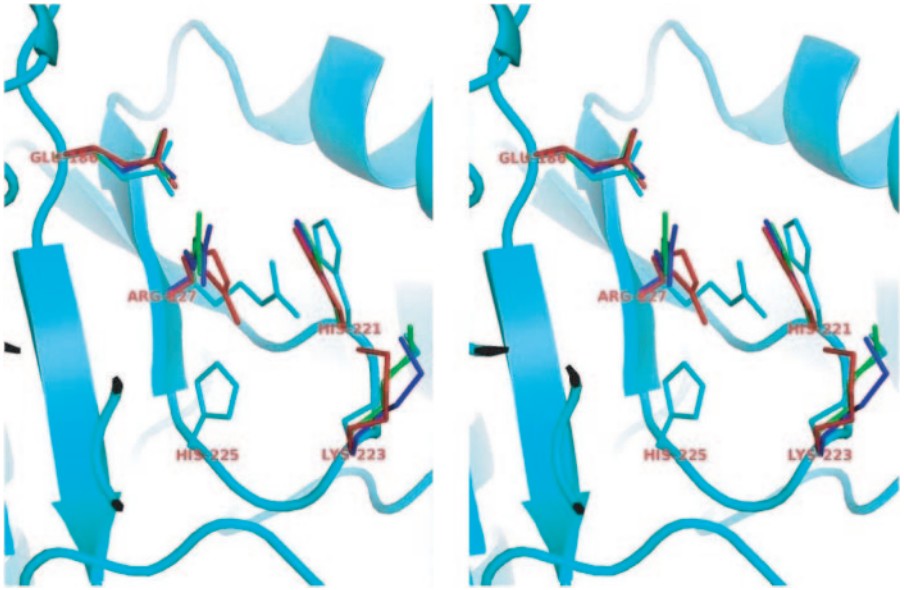

FIG. 4. Structural changes upon nucleotide binding. The images show stereoviews of the superposition of residues in the active site from the structures of native NSP2 (cyan), H225A NSP2 (red), H225A NSP2 plus AMPPNP (green), and H225A NSP2 plus ATP–γ-S (blue). The major changes are seen with Arg 227.

electron density for the Ala residue at position 225, confirming the mutation. The only noticeable structural change correlating with the H225A mutation is in the side chain of Arg227 in the active-site cleft (Fig. 4). In the native structure, the side chain of this residue is positioned between His225 and His221, whereas in the mutant, this side chain has moved closer to Ala225. Comparison of electron density maps of the H225A mutant and its complexes with either the ATP analog AMPPNP (Fig. 3A) or ATP–γ-S (Fig. 3B) showed strong electron density (>4σ) corresponding to the three phosphates of the nucleotide. However, in both nucleotide-bound structures, the electron density for the sugar was weak and that for the base was absent, indicating that the base was not held in place by any specific interactions with NSP2 and that the base has a considerable degree of freedom in its orientation with respect to the sugar and phosphate. This is consistent with the observation that NSP2 is a general NTPase with no specificity for a particular base (40).

Change in protein conformation upon nucleotide binding. Although the overall conformations of NSP2 in the phosphohistidine and nucleotide-bound structures do not differ significantly (average RMSD of 0.6 Å for matching C-α atoms), there are small conformational changes consistently seen at specific locations in these structures. These include a slight movement of the C-terminal domain towards the N-terminal domain, a more noticeable shift in the loop formed from residues 12 to 18 (even though this loop is away from the active-site cleft), and a significant conformational change in the side chain orientation of Arg227. In the native structure, the side chain position of Arg227 is positioned such that it would prevent the γ-phosphate of the nucleotide from reaching the catalytic histidine. In the nucleotide-bound structure, this side chain is reoriented, making space for the nucleotide to approach and interact with His225 (Fig. 4). At the new position, N-ε of Arg227 forms a hydrogen bond with the side chain carboxyl oxygen of Glu186. In the case of native NSP2 as well as the noncomplexed H225A mutant, the side chain of Arg227 is too far from Glu186 to allow such hydrogen bonding.

Nucleotide-protein interactions at the active site. In H225A NSP2 complexes with AMPPNP or ATP–γ-S, the nucleotide is held in the active-site cleft through a series of hydrogen-bonding interactions between the three phosphates of the nucleotide, the side chain atoms of the protein, and a number of water molecules (Fig. 5A and B). Residues His221, Lys223, Arg227, and Lys188 form hydrogen bonds with the oxygen atoms of the three phosphates, thereby orienting the phosphate groups and positioning the γ-phosphate close to residue 225. The side chain of Arg227, which undergoes a significant change in orientation upon nucleotide binding to NSP2, is held in place by hydrogen bonding with Glu186 so that the terminal nitrogen atoms of Arg227 can then interact with the nucleotide. The NH1 group of Arg227 forms a hydrogen bond with one of the oxygen atoms of the γ-phosphate and a water molecule, whereas the NH2 group forms a hydrogen bond with an oxygen atom of the α-phosphate. The side chains of residues Lys188 and Lys223 interact with the oxygen atoms of the γ- and β-phosphates, respectively. Similar interactions are also present in the complex with AMPPNP. However, there are small alterations reflecting the differences in the chemical structures of the two ATP analogues. In the H225A NSP2–ATP–γ-S structure, the N-δ atom of His221 makes a hydrogen bond with the bridging oxygen atom between the β- and γ-phosphates, whereas in the H225A NSP2-AMPPNP structure, because this bridging oxygen atom is replaced by nitrogen in AMPPNP, N-δ of His221 hydrogen bonds instead to the bridging oxygen atom between the α- and β-phosphates.

NSP2 exhibits NDP kinase-like activity. These results show that NTP hydrolysis by NSP2 involves the formation of a relatively stable phosphohistidine intermediate that can be trapped in crystals. Such an intermediate has been visualized in

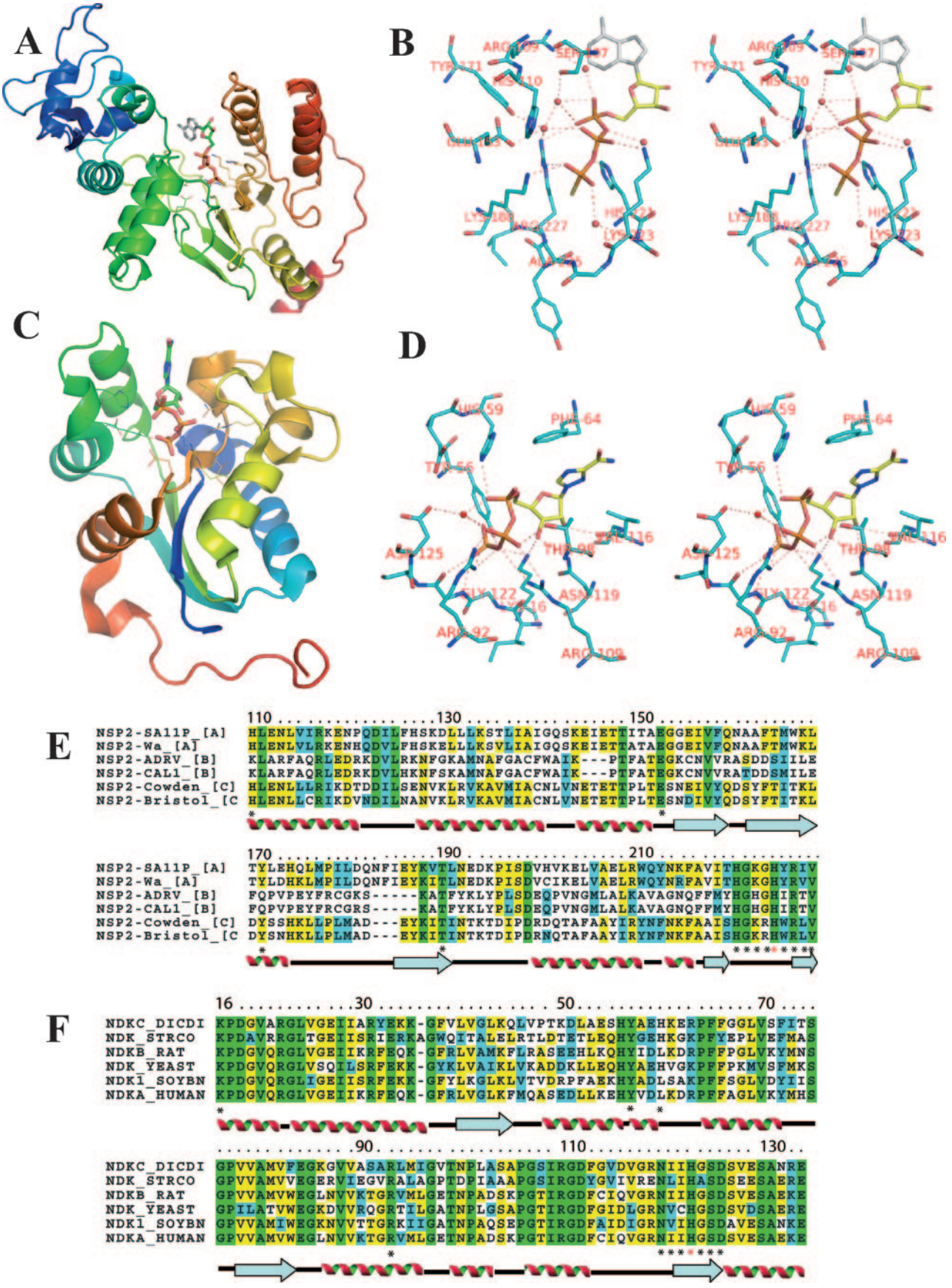
A
B
C
D
E
NSP2-SA11P_[A]
NSP2-Wa_[A]
NSP2-ADRV_[B]
NSP2-CAL1_[B]
NSP2-Cowden_[C]
NSP2-Bristol_[C
F
NDKC_DICDI
NDK_STRCO
NDKB_RAT
NDK_YEAST
NDK1_SOYBN
NDKA_HUMAN

phosphotransferases such as cellular NDP kinases, by which the transfer of γ-phosphate from an NTP donor to an NDP acceptor occurs (16, 24). This prompted us to investigate whether NSP2 exhibited NDP kinase activity.

One of the most sensitive approaches for measuring NDP kinase activity is the real-time bioluminometric assay (19), a luciferin-luciferase-based system that detects the formation of ATP in reaction mixtures containing ADP and another NTP (e.g., GTP, UTP, or CTP) in the presence of an NDP kinase. In initial experiments, native NSP2 and H225A NSP2 were tested for NDP kinase-like activity in reaction mixtures containing 20 mM Tris-HCl (pH 7.5), 4 mM $MgCl_2$, 1.0 mM UTP, 1.0 mM ADP, and 2 μM of the recombinant protein. Reaction mixtures containing native NSP2 showed a linear increase in the concentration of ATP with time, whereas mixtures containing the active-site mutant H225A NSP2 showed no formation of ATP with time (Fig. 6A). These results indicate that NSP2 indeed possesses NDP kinase activity, catalyzing the formation of ATP in reaction mixtures containing ADP and UTP, and that the activity is completely abolished when the catalytic histidine is mutated to alanine.

To determine the kinetic parameters of this activity, we carried out a series of experiments with ADP as the phosphate acceptor and GTP, UTP, or CTP as the phosphate donor and measured the rate of formation of ATP as a function of nucleotide concentration. The reciprocal plot of $1/v$ versus 1/[GTP] at different fixed concentrations of ADP showed a set of parallel lines (Fig. 6B) typical of a ping-pong reaction mechanism (36). With this type of mechanism, the apparent K_m value for one substrate increases as the other substrate approaches the saturating concentration. The true kinetic parameters for one substrate can thus be determined when the other substrate is present at saturating concentrations. Therefore, to obtain kinetic parameters with UTP as the phosphate donor, the rate of ATP formation was measured in reaction mixtures containing various levels of UTP and a saturating concentration of ADP (1.5 mM) (Fig. 6C). The k_{cat} and K_m values calculated from plots of UTP concentration versus ATP formation were 0.27 min^{-1} and 215 μM, respectively. In the experiment with a saturating concentration of UTP and various ADP concentrations, the corresponding values for ADP (Fig. 6D) were 0.33 min^{-1} and 350 μM, respectively. The kinetic parameters determined for other NTPs, such as GTP and CTP, were similar to those for UTP (data not shown), indicating a lack of base specificity, a feature that is generally observed with cellular NDP kinases. These results are consistent with previous results showing that NTP hydrolysis by NSP2 is not base specific (40).

DISCUSSION

Of the 12 proteins encoded by the rotavirus genome, NSP2 is the only one known to exhibit NTPase activity. In many viral systems, NTPase activity is implicated in genome replication and packaging, particularly in association with helicase activity, in which the hydrolysis of NTP is used for energy transduction. The structures of several viral helicases have been determined, and they all show similarities with cellular helicases, enzymes which are essential for processes such as DNA replication, repair, recombination, transcription, splicing, and translation (12, 44). Several characteristics of NSP2, such as its octameric self-assembly, its lack of recognizable helicase motifs (e.g., Walker A or B motifs), its lack of significant conformational change upon nucleotide binding and cleavage, its use of a histidine as a catalytic residue, and its formation of a relatively stable phosphohistidine intermediate during catalysis, clearly distinguish NSP2 from typical helicases, suggesting that the function of the NTPase activity of NSP2 is something other than energy transduction.

Nucleotide binding and NTP hydrolysis—comparison with HIT proteins. The organization and positioning of the nucleotide binding site and catalytic histidine in NSP2 are remarkably consistent with earlier predictions based on the structural similarity of NSP2 with the HIT proteins (17). However, the modes of nucleotide binding and hydrolysis appear to differ significantly between NSP2 and HIT proteins. The catalytic histidine in HIT proteins is nucleotidylated during catalysis by covalent attachment of the α-phosphate of the nucleotide. In contrast, the catalytic histidine (His225) in NSP2 is phosphorylated by covalent attachment of the γ-phosphate of the nucleotide. Consequently, the disposition of residues at the active sites of NSP2 and HIT proteins is different. In particular, the bridging oxygen between the β- and γ-phosphates of the nucleotide bound to NSP2 makes a hydrogen bond with His221 that seems to play a crucial role during catalysis. In HIT proteins, a serine residue performs the equivalent function to that of NSP2 His221 in stabilizing the bridging oxygen (23). During catalysis of both NSP2 and HIT proteins, the nucleotide phosphate becomes covalently attached to the N-ε position of the catalytic histidine. However, in the case of HIT proteins, the

FIG. 5. NSP2 is distinct from cellular NDP kinases in both structure and catalytic mechanism. (A) Ribbon diagram of NSP2, shown in rainbow colors from N- to C-terminal residues, with a nucleotide bound in the active-site cleft. (B) Stereo diagram of active-site residues and bound ATP–γ-S in the H225A NSP2 complex structure. The base of the nucleotide (gray) was not modeled from the electron density map and is only proposed. (C) Ribbon diagram of a prototype NDP kinase (*Dictyostelium discoideum*), shown in rainbow colors from N- to C-terminal residues, with a bound nucleotide (PDB file 1mn9). (D) Stereo diagram of the active-site residues and a bound ribavirin triphosphate (RTP) in the same NDP kinase structure (1mn9). In this particular structure, the catalytic residue His122 is mutated to Gly. (E) Sequence alignment of NSP2 proteins from group A rotaviruses SA11-P (simian strain) and Wa (human), group B rotaviruses ADRV and CAL1 (human), and group C rotaviruses Cowden (bovine) and Bristol (human) (GenBank accession numbers AAA47298, AAA47301, AAA47328, AAF72868, CAA46742, and AJ132205, respectively). Residue positions correspond to those of the SA11-P sequence. (F) Sequence conservation of NDP kinases across different species. DICDI, *Dictyostelium discoideum* (slime mold); STRCO, *Streptomyces coelicolor*; RAT, *Rattus norvegicus*; YEAST, *Saccharomyces cerevisiae* (baker's yeast); SOYBN, glycine max soybean; and HUMAN, *Homo sapiens*. Residue positions correspond to those of the *D. discoideum* sequence. Strictly conserved residues across the sequences, partially conserved residues, and similar residues are shaded in green, yellow, and cyan, respectively. Active-site residues and the catalytic histidine are denoted by black and red asterisks, respectively. Secondary structural elements are indicated below the sequences.

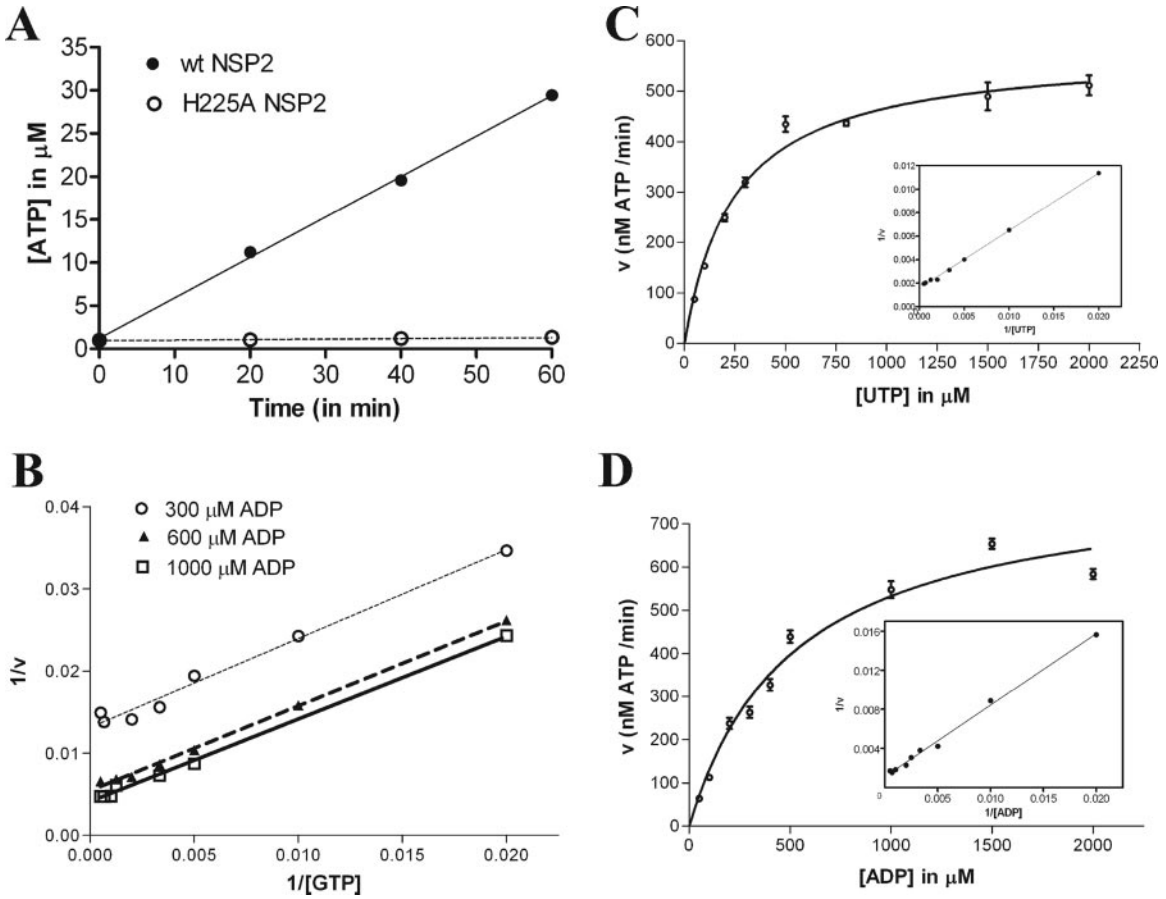

FIG. 6. NDP kinase activity of NSP2, detected using a luciferin-luciferase assay system. (A) Formation of ATP over time in reaction mixtures containing 20 mM Tris-HCl (pH 7.5), 4 mM $MgCl_2$, 1.0 mM UTP, 1.0 mM ADP, and 2 μM native or H225A mutant NSP2. (B) Kinetics of NDP kinase activity. Data for a Lineweaver-Burk plot were obtained at room temperature by varying the concentration of GTP at different fixed concentrations of ADP. (C) Enzyme kinetics at 37°C with various concentrations of UTP and a fixed concentration of ADP (1.5 mM). (D) Enzyme kinetics at 37°C with various concentrations of ADP and a fixed concentration of UTP (1.5 mM). For panels B to D, the reactions were carried out in 20 mM Tris-HCl (pH 7.5) containing 4 mM $MgCl_2$ and were started by the addition of NSP2 to a final concentration of 2 μM. The reaction rate was obtained by measuring the concentration of ATP at different times (0, 10, 20, 30, and 40 min). The kinetic parameters V_{max} and K_m were obtained by reciprocal (Lineweaver-Burk) plots, shown in the insets of panels C and D.

N-δ atom of the catalytic histidine is hydrogen bonded to main-chain carbonyl oxygen, whereas in NSP2, the same atom is hydrogen bonded to a water molecule. Another important contrasting feature is that catalysis is a Mg^{2+}-independent event for HIT proteins, but for NSP2, a divalent metal ion is essential for catalysis, a characteristic also shared with NDP kinases. Our studies provide an example of how a viral protein using the same fold as ubiquitous cellular proteins acquires a functionally distinct enzymatic activity by incorporating appropriate changes into the amino acid sequence. A proposed mechanism for the NTPase activity of NSP2, based on our structural observations, is given in Fig. 7. We envisage that the catalytic mechanism of the recently demonstrated RTPase activity of NSP2 (46), in which the terminal phosphate is cleaved from a pppRNA substrate, is similar to that of NTPase activity involving the same His225 residue.

Comparison of NSP2 with cellular NDP kinases. Our studies show that NSP2 exhibits several signature features of cellular NDP kinases, including the use of histidine as a catalytic residue, formation of a relatively stable phosphohistidine intermediate, and the ability to transfer a covalently linked phosphate group to an NDP. Cellular NDP kinases are well-characterized enzymes, typically consisting of ~150 residues that display a high degree of sequence and structural conservation. NSP2 bears no resemblance to these cellular enzymes either in its primary sequence or in its structure (Fig. 5A to D). For instance, the sequence surrounding the catalytic His ([H]) of NSP2 (HGKG[H]YRIV) is very different from the sequence surrounding the catalytic His of cellular NDP kinases (NII[H]GSD) (Fig. 5E and F). In addition, the modes of nucleotide binding are also different in these proteins. In all cellular NDP kinases, the bound nucleotide adopts a strained conformation in which the β-phosphate folds back toward the sugar to facilitate a hydrogen-bonding interaction between the 3′-OH group of the sugar and the bridging oxygen atom between the β- and γ-phosphates (16) (Fig. 5D). This interaction with the 3′-OH group plays a crucial role in catalysis by protonating the leaving group. Modification of this group severely hinders kinase activity (33). In NSP2, however, the phosphates of the bound nucleotide adopt an extended conformation in

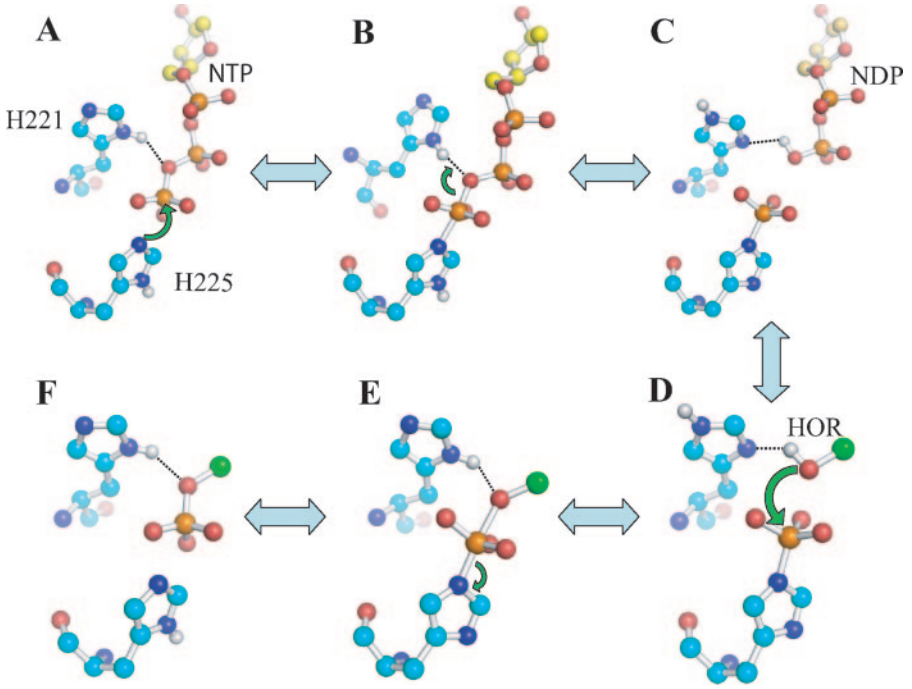

FIG. 7. Proposed catalytic mechanism of NSP2. (A) N-δ of His225 forms a hydrogen bond with a water molecule (not shown here), and N-ε attacks the P-γ atom of the NTP. This results in the formation of a pentavalent transition state (B) which, being unstable, dissociates to form a phosphohistidine intermediate and ADP (C). The dissociation of the pentavalent transition state is assisted by His221, which donates a proton attached to its N-δ atom to the bridging oxygen atom between the β- and γ-phosphates of the nucleotide and neutralizes the charge that would otherwise develop on the leaving group. The relatively stable phosphohistidine intermediate would allow the NDP product to diffuse out of the active-site cleft. Subsequently, a nucleophilic oxygen atom associated with (i) a water molecule (NTPase activity), (ii) the terminal phosphate of a second NDP (NDP kinase activity), or (iii) a serine or threonine residue of a different protein (phosphotransferase activity) attacks the P atom of the phosphohistidine intermediate, assisted again by His221 (D). This leads to the formation of a pentavalent transition state (E) which, being unstable, releases the product, i.e., a free phosphate in the case of NTP hydrolysis, an NTP in the case of NDP kinase activity, or a phosphoamino acid in the case of phosphoryl-transferase activity (F).

which the same bridging oxygen atom is hydrogen bonded to His221, an interaction that may play a role equivalent to that of the 3′-OH group in cellular NDP kinases (Fig. 7). Another significant difference between NSP2 and cellular NDP kinases is in the orientation of the imidazole ring of the catalytic histidine, a feature allowing phosphorylation to take place at the N-δ position in cellular NDP kinases versus the N-ε position in NSP2. In toto, these differences clearly indicate that NSP2 is distinct from the highly conserved cellular NDP kinases.

Catalytic site residues are conserved in NSP2. In addition to His225 and His221, our structural studies implicate Lys223, Arg227, and Lys188 in the catalytic activity of NSP2. Are these residues conserved among different strains of rotavirus? Rotaviruses are classified into three groups, A, B, and C, which are antigenically and genetically distinct (13). The NSP2 species analyzed in our study is from a group A rotavirus (simian strain). Despite some variation in the overall sequences of NSP2 proteins from different groups, the residues important for catalytic activity are highly conserved (Fig. 5E). A recently determined X-ray structure of NSP2 from a human group C rotavirus (Bristol strain) shows structural features similar to those of group A NSP2, including the polypeptide fold, domain organization, and disposition of the residues important for catalytic activity (41). Thus, it is very likely that the NTPase and associated NDP kinase activities of NSP2 are evolutionarily conserved in rotaviruses. The highly conserved catalytic pocket, which is distinct from that of cellular NDP kinases, represents an excellent target for designing broad-spectrum antiviral drugs against rotavirus infections.

Kinetic parameters of NDP kinase activity of NSP2. Although the K_m value for the NDP kinase activity of NSP2 is similar to those of cellular NDP kinases, the overall catalytic efficiency is significantly lower than that normally seen with cellular NDP kinases. As a consequence, we considered the possibility that the NDP kinase activity detected for NSP2 simply represents a trivial reverse reaction of its NTPase activity. However, two observations suggest that this is not the case. Firstly, the k_{cat} (0.27 min^{-1}) value for the NDP kinase activity of NSP2 is an order of magnitude greater than that of its NTPase activity (0.018 min^{-1}), indicating that NDPs are preferred substrates compared to water. Secondly, in our assays we clearly observed that the γ-phosphate from an NTP (GTP or UTP in our studies) is transferred to an NDP (ADP) with a different base composition, thus negating the possibility of an off-and-on movement of the γ-P on the same nucleotide.

In general, the k_{cat} values for the various enzymatic activities of NSP2 are particularly low compared to those of typical enzymes. Perhaps the NSP2 activities are stimulated to levels more likely to be considered biological through its interaction with other viral proteins, such as the phosphoprotein NSP5, the polymerase VP1, or the inner capsid protein VP2. The

GTPase of the Ras superfamily of proteins is a good example of an enzyme with a low intrinsic k_{cat} value (0.02 min^{-1}) that is markedly stimulated by interaction with another protein, in this case the GTPase-activating protein (5). Alternatively, the low activity levels of NSP2 may be compensated by the presence of high concentrations of the protein in the viroplasm. With a k_{cat} value of 0.27 min^{-1}, a 1 mM concentration of NSP2 could hypothetically generate a 270 μM concentration of NTPs per minute inside each viroplasm. Such a rate is significant considering that the average intracellular NTP concentration is ~1,000 μM (4). Although the precise concentration of NSP2 in the viroplasm is not known, a concentration in the millimolar range is not unrealistic considering that NSP2 is a high-copy-number protein accumulating nearly exclusively in viroplasms and that the protein components are tightly packed in these electron-dense structures, which are typically a micrometer wide (10).

Functional role of NSP2 enzymatic activities in rotavirus genome replication. While the ssRNA-binding and helix-destabilizing activities of NSP2 have been suggested to relax positive-strand RNA templates in preparation for dsRNA synthesis (42), rationalizing the roles of the enzymatic activities of NSP2 (i.e., NTPase, RTPase, and NDP kinase activities) in virus replication is much more challenging. However, the importance of these activities, all of which share the same catalytic site centered around the critical H225, in rotavirus genome replication is clearly underscored by in vivo complementation experiments which show that the H225A mutant of NSP2 fails to support dsRNA synthesis without affecting viroplasm formation (41). A good example of a well-characterized viral nonstructural protein that exhibits both NTPase and RTPase activities is flavivirus NS3 (47). The NTPase activity of NS3 was clearly shown to be associated with a helicase function, and its RTPase activity is implicated in removal of the γ-P from positive-sense RNA and its subsequent capping. Despite similar enzymatic activities, NSP2, with its HIT-like fold, appears to be both functionally and structurally distinct from NS3.

An unusual aspect of the rotavirus genome is that the γ-P is missing from the 5′ end of the negative-strand RNA (15, 29). Because NSP2 is associated with replication intermediates actively synthesizing dsRNA (2), suggestions have been made that the γ-P is removed from nascent negative-strand RNAs via the RTPase activity of NSP2. Unlike the negative-strand RNA, the positive strand is capped, a modification that prevents its attack by the RTPase activity (46). The capping of the positive-sense RNA in rotavirus is carried out by a minor structural protein, VP3, during endogenous transcription (9). Based on X-ray crystallographic studies of the reovirus polymerase (39), negative-strand synthesis from the positive-strand template generates a dsRNA product within the catalytic core of the enzyme, which then leaves the polymerase in the same dsRNA form. Because dsRNAs are not substrates for the RTPase activity of NSP2, it is difficult to understand how NSP2 could be responsible for the removal of the γ-P from the negative-strand RNA and how this activity per se could be linked directly to dsRNA synthesis. Nonetheless, the different combination of catalytic activities noted for NSP2 raises the possibility that the protein could have multiple enzymatic functions, switching from one activity to another depending on its interactions with ligands. Given that the functional form of NSP2 is an octamer capable of simultaneously displaying active sites, NSP2 may in fact be able to concurrently carry out different catalytic activities.

Possible role of NDP kinase activity in the homeostasis of nucleotide pools. Although further studies are clearly required, one use of the NDP kinase activity of NSP2 may be to regulate nucleotide pools in the viroplasm such that they are sufficient to support genome transcription and replication by the viral polymerase (37). Adequate concentrations of nucleotides are also necessary for promoting the fidelity and processivity of viral RNA synthesis. The need for nucleotides in the viroplasm extends beyond RNA polymerization to include a source of hydrolyzable ATP for transcription (38), NSP5 phosphorylation, and possibly energy-demanding steps, such as RNA packaging and translocation. As a result, the NDP kinase activity of NSP2 may be vital to compensating for the drawdown of ATP in the viroplasm by providing a mechanism for using GTP, CTP, and UTP to convert ADP to ATP. Given such demand for nucleotides, it may be reasoned that rotavirus, with its large genome (~18 kilobases), may have evolved specialized biosynthetic pathways to counter possible imbalances in the intracellular nucleotide levels occurring during virus replication and to regulate these levels appropriately within viroplasms. Abrogation of dsRNA synthesis, as observed with the H225A mutant (41), could be due in part to the absence of this activity.

With the data currently available, the question of whether other proteins in the viroplasm could be substrates for the phosphotransfer activity of NSP2 remains open. While this is a possibility, it would require the acceptor region of the protein to gain access to the H225 catalytic residue, a complex feat given that this residue is positioned deep within the active-site cleft. Potential substrates of the phosphoryl-transfer activity could include cellular proteins, although no such proteins have been demonstrated to exist within the viroplasm. Of the viral proteins, the most likely substrate for the phosphoryl-transfer activity is NSP5, the binding partner of NSP2 in viroplasm formation. NSP5 is a serine- and threonine-rich protein that exists as a set of phosphorylated isomers in the infected cell, ranging from a 28-kDa hypophosphorylated form to 32- to 34-kDa hyperphosphorylated forms (1). However, recent studies suggest that the catalytic activity of NSP2 is not involved in the phosphorylation of NSP5. Specifically, these studies have revealed that NSP5 expressed alone in uninfected cells undergoes hypophosphorylation (8). However, when it is coexpressed with NSP2, including mutant species of NSP2 that are NTPase defective, NSP5 undergoes hyperphosphorylation. Thus, the phosphorylation of NSP5, although stimulated in vivo by NSP2, appears to proceed independently of the NTPase activity of NSP2. Multiple lines of evidence have indicated that cellular casein kinase-like enzymes mediate the hyperphosphorylation of NSP5 (11).

In summary, in addition to providing structural insights into nucleotide binding and the catalytic mechanism of triphosphatase activity in rotavirus NSP2, our studies show that NSP2 also exhibits NDP kinase-like activity. Earlier studies have reported NDP kinase activity for replication complexes of other viruses, such as encephalomyocarditis virus (21), reovirus (34), and vesicular stomatitis virus (43). These studies, however, did not specifically identify the viral protein(s) responsi-

ble for this activity. The utility of an NDP kinase activity for homeostasis of nucleotide pools during genome replication has been suggested for encephalomyocarditis virus (21, 22) and needs to be examined further for rotavirus. From the perspective of structure-activity relationships, our studies on NSP2 provide a unique illustration of how the same protein fold can be utilized to perform different enzymatic functions and, conversely, how the same catalytic function can be performed by proteins with entirely different folds. An interesting question is whether the fold similarity between NSP2 and HIT proteins is a consequence of divergent or convergent evolution. The absence of any noticeable sequence similarity, the lack of a classical HIT motif in NSP2, and the contrasting enzymatic functions of NSP2 and HIT proteins suggest that the HIT fold in rotavirus NSP2 resulted from convergent evolution. Indeed, this is consistent with recent suggestions that some members of the HIT superfamily of proteins evolved their shared features not by divergent evolution but, instead, by convergent evolution (20). However, it remains possible that all of the HIT proteins evolved from a common ancestral smaller nucleotide binding fold that has served as the basic building block for the evolution of more complex and divergent structures with differing activities.

ACKNOWLEDGMENTS

We thank M. K. Estes, R. F. Ramig, and H. F. Gilbert for many helpful discussions and S. S. Chirala for help with the bioluminometric assay. We also thank the staff of the SBC-CAT 19ID beamline at the Advanced Photon Source (supported by the U.S. Department of Energy, Basic Energy Sciences, and Office of Science) for their help during data collection.

We acknowledge support from NIH grants AI36040 (to B.V.V.P.) and GM069769 (to R.J.), by the Intramural Research Program of the National Institute of Allergy and Infectious Diseases, NIH (to R.V.D.C., Z.F.T., and J.T.P.), and by the Welch Foundation (to B.V.V.P.).

REFERENCES

1. **Afrikanova, I., M. C. Miozzo, S. Giambiagi, and O. Burrone.** 1996. Phosphorylation generates different forms of rotavirus NSP5. J. Gen. Virol. **77:** 2059–2065.
2. **Aponte, C., D. Poncet, and J. Cohen.** 1996. Recovery and characterization of a replicase complex in rotavirus-infected cells by using a monoclonal antibody against NSP2. J. Virol. **70:**985–991.
3. **Bird, L. E., H. S. Subramanya, and D. B. Wigley.** 1998. Helicases: a unifying structural theme? Curr. Opin. Struct. Biol. **8:**14–18.
4. **Bochner, B. R., and B. N. Ames.** 1982. Complete analysis of cellular nucleotides by two-dimensional thin layer chromatography. J. Biol. Chem. **257:** 9759–9769.
5. **Bourne, H. R., D. A. Sanders, and F. McCormick.** 1991. The GTPase superfamily: conserved structure and molecular mechanism. Nature **349:**117–127.
6. **Brenner, C.** 2002. Hint, Fhit, and GalT: function, structure, evolution, and mechanism of three branches of the histidine triad superfamily of nucleotide hydrolases and transferases. Biochemistry **41:**9003–9014.
7. **Brunger, A. T., P. D. Adams, G. M. Clore, W. L. DeLano, P. Gros, R. W. Grosse-Kunstleve, J. S. Jiang, J. Kuszewski, M. Nilges, N. S. Pannu, R. J. Read, L. M. Rice, T. Simonson, and G. L. Warren.** 1998. Crystallography & NMR system: a new software suite for macromolecular structure determination. Acta Crystallogr. D **54:**905–921.
8. **Carpio, R. V., F. D. Gonzalez-Nilo, H. Jayaram, E. Spencer, B. V. Prasad, J. T. Patton, and Z. F. Taraporewala.** 2004. Role of the histidine triad-like motif in nucleotide hydrolysis by the rotavirus RNA-packaging protein NSP2. J. Biol. Chem. **279:**10624–10633.
9. **Chen, D., C. L. Luongo, M. L. Nibert, and J. T. Patton.** 1999. Rotavirus open cores catalyze 5′-capping and methylation of exogenous RNA: evidence that VP3 is a methyltransferase. Virology **265:**120–130.
10. **Eichwald, C., J. F. Rodriguez, and O. R. Burrone.** 2004. Characterization of rotavirus NSP2/NSP5 interactions and the dynamics of viroplasm formation. J. Gen. Virol. **85:**625–634.
11. **Eichwald, C., F. Vascotto, E. Fabbretti, and O. R. Burrone.** 2002. Rotavirus NSP5: mapping phosphorylation sites and kinase activation and viroplasm localization domains. J. Virol. **76:**3461–3470.
12. **Eoff, R. L., and K. D. Raney.** 2005. Helicase-catalysed translocation and strand separation. Biochem. Soc. Trans. **33:**1474–1478.
13. **Estes, M. K.** 2001. Rotaviruses and their replication, p. 1747–1785. *In* D. M. Knipe, P. M. Howley, D. E. Griffin, R. A. Lamb, M. A. Martin, B. Roizman, and S. E. Straus (ed.), Fields virology, 4th ed. Lippincott Williams & Wilkins, Philadelphia, PA.
14. **Fabbretti, E., I. Afrikanova, F. Vascotto, and O. R. Burrone.** 1999. Two non-structural rotavirus proteins, NSP2 and NSP5, form viroplasm-like structures in vivo. J. Gen. Virol. **80:**333–339.
15. **Imai, M., K. Akatani, N. Ikegami, and Y. Furuichi.** 1983. Capped and conserved terminal structures in human rotavirus genome double-stranded RNA segments. J. Virol. **47:**125–136.
16. **Janin, J., C. Dumas, S. Morera, Y. Xu, P. Meyer, M. Chiadmi, and J. Cherfils.** 2000. Three-dimensional structure of nucleoside diphosphate kinase. J. Bioenerg. Biomembr. **32:**215–225.
17. **Jayaram, H., Z. Taraporewala, J. T. Patton, and B. V. Prasad.** 2002. Rotavirus protein involved in genome replication and packaging exhibits a HIT-like fold. Nature **417:**311–315.
18. **Jones, T. A., J. Y. Zou, S. W. Cowan, and Kjeldgaard.** 1991. Improved methods for building protein models in electron density maps and the location of errors in these models. Acta Crystallogr. A **47:**110–119.
19. **Karamohamed, S., T. Nordstrom, and P. Nyren.** 1999. Real-time bioluminometric method for detection of nucleoside diphosphate kinase activity. BioTechniques **26:**728–734.
20. **Kijas, A. W., J. L. Harris, J. M. Harris, and M. F. Lavin.** 2006. Aprataxin forms a discrete branch in the HIT (histidine triad) superfamily of proteins with both DNA/RNA binding and nucleotide hydrolase activities. J. Biol. Chem. **281:**13939–13948.
21. **Koonin, E. V., and V. I. Agol.** 1984. Encephalomyocarditis virus replication complexes preferentially utilizing nucleoside diphosphates as substrates for viral RNA synthesis. Nucleotide kinases specifically associated with the complex channel RNA precursor. Eur. J. Biochem. **144:**249–254.
22. **Koonin, E. V., and V. I. Agol.** 1983. Encephalomyocarditis virus replication complexes that prefer nucleoside diphosphates as substrates for viral RNA synthesis. Virology **129:**309–318.
23. **Krakowiak, A., H. C. Pace, G. M. Blackburn, M. Adams, A. Mekhalfia, R. Kaczmarek, J. Baraniak, W. J. Stec, and C. Brenner.** 2004. Biochemical, crystallographic, and mutagenic characterization of hint, the AMP-lysine hydrolase, with novel substrates and inhibitors. J. Biol. Chem. **279:**18711–18716.
24. **Lascu, I., and P. Gonin.** 2000. The catalytic mechanism of nucleoside diphosphate kinases. J. Bioenerg. Biomembr. **32:**237–246.
25. **Lasker, M., C. D. Bui, P. G. Besant, K. Sugawara, P. Thai, G. Medzihradszky, and C. W. Turck.** 1999. Protein histidine phosphorylation: increased stability of thiophosphohistidine. Protein Sci. **8:**2177–2185.
26. **Levin, M. K., and S. S. Patel.** 2003. Helicases as molecular motor. *In* M. Schliwa (ed.), Molecular motors. Wiley-VCH Verlag GmbH, Weinheim, Germany.
27. **Lima, C. D., M. G. Klein, and W. A. Hendrickson.** 1997. Structure-based analysis of catalysis and substrate definition in the HIT protein family. Science **278:**286–290.
28. **McCoy, A. J., R. W. Grosse-Kunstleve, L. C. Storoni, and R. J. Read.** 2005. Likelihood-enhanced fast translation functions. Acta. Crystallogr. D **61:**458–464.
29. **McCrae, M. A., and J. G. McCorquodale.** 1983. Molecular biology of rotaviruses. V. Terminal structure of viral RNA species. Virology **126:**204–212.
30. **Patton, J. T., L. S. Silvestri, M. A. Tortorici, R. Vasquez-Del Carpio, and Z. F. Taraporewala.** 2006. Rotavirus genome replication and morphogenesis: role of the viroplasm. Curr. Top. Microbiol. Immunol. **309:**169–187.
31. **Pflugrath, J. W.** 1999. The finer things in X-ray diffraction data collection. Acta Crystallogr. D **55:**1718–1725.
32. **Prasad, B. V., R. Rothnagel, C. Q. Zeng, J. Jakana, J. A. Lawton, W. Chiu, and M. K. Estes.** 1996. Visualization of ordered genomic RNA and localization of transcriptional complexes in rotavirus. Nature **382:**471–473.
33. **Schneider, B., Y. W. Xu, J. Janin, M. Veron, and D. Deville-Bonne.** 1998. 3′-Phosphorylated nucleotides are tight binding inhibitors of nucleoside diphosphate kinase activity. J. Biol. Chem. **273:**28773–28778.
34. **Schochetman, G., and S. Millward.** 1972. Ribonucleoside diphosphate precursors for in vitro reovirus RNA synthesis. Nat. New Biol. **239:**77–79.
35. **Schuck, P., Z. Taraporewala, P. McPhie, and J. T. Patton.** 2001. Rotavirus nonstructural protein NSP2 self-assembles into octamers that undergo ligand-induced conformational changes. J. Biol. Chem. **276:**9679–9687.
36. **Segel, I. H.** 1975. Enzyme kinetics, behavior and analysis of rapid equilibrium and steady-state enzyme systems. John Wiley & Sons, New York, NY.
37. **Silvestri, L. S., Z. F. Taraporewala, and J. T. Patton.** 2004. Rotavirus replication: plus-sense templates for double-stranded RNA synthesis are made in viroplasms. J. Virol. **78:**7763–7774.
38. **Spencer, E., and M. L. Arias.** 1981. In vitro transcription catalyzed by heat-treated human rotavirus. J. Virol. **40:**1–10.
39. **Tao, Y., D. L. Farsetta, M. L. Nibert, and S. C. Harrison.** 2002. RNA

synthesis in a cage—structural studies of reovirus polymerase lambda3. Cell **111:**733–745.

40. **Taraporewala, Z., D. Chen, and J. T. Patton.** 1999. Multimers formed by the rotavirus nonstructural protein NSP2 bind to RNA and have nucleoside triphosphatase activity. J. Virol. **73:**9934–9943.
41. **Taraporewala, Z. F., X. Jiang, R. Vasquez-Del Carpio, H. Jayaram, B. V. Prasad, and J. T. Patton.** 2006. Structure-function analysis of rotavirus NSP2 octamer by using a novel complementation system. J. Virol. **80:**7984–7994.
42. **Taraporewala, Z. F., and J. T. Patton.** 2001. Identification and characterization of the helix-destabilizing activity of rotavirus nonstructural protein NSP2. J. Virol. **75:**4519–4527.
43. **Testa, D., and A. K. Banerjee.** 1979. Nucleoside diphosphate kinase activity in purified cores of vesicular stomatitis virus. J. Biol. Chem. **254:**9075–9079.
44. **Tuteja, N., and R. Tuteja.** 2004. Prokaryotic and eukaryotic DNA helicases. Essential molecular motor proteins for cellular machinery. Eur. J. Biochem. **271:**1835–1848.
45. **Valenzuela, S., J. Pizarro, A. M. Sandino, M. Vasquez, J. Fernandez, O. Hernandez, J. Patton, and E. Spencer.** 1991. Photoaffinity labeling of rotavirus VP1 with 8-azido-ATP: identification of the viral RNA polymerase. J. Virol. **65:**3964–3967.
46. **Vasquez-Del Carpio, R., F. D. Gonzalez-Nilo, G. Riadi, Z. F. Taraporewala, and J. T. Patton.** 2006. Histidine triad-like motif of the rotavirus NSP2 octamer mediates both RTPase and NTPase activities. J. Mol. Biol. **362:**539–554.
47. **Yon, C., T. Teramoto, N. Mueller, J. Phelan, V. K. Ganesh, K. H. Murthy, and R. Padmanabhan.** 2005. Modulation of the nucleoside triphosphatase/RNA helicase and 5′-RNA triphosphatase activities of dengue virus type 2 nonstructural protein 3 (NS3) by interaction with NS5, the RNA-dependent RNA polymerase. J. Biol. Chem. **280:**27412–27419.